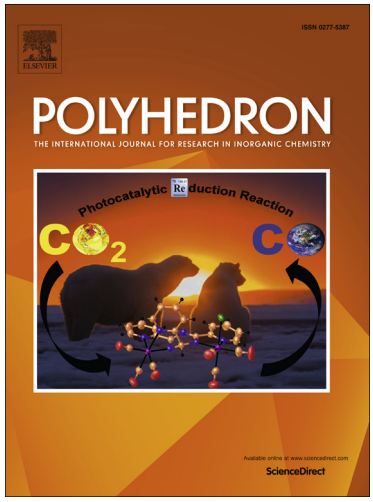

Ruthenium Complexes of Diphenylphosphino Derivatives of Carboxylic Amides: Synthesis and Characterization of bidentate P,N- and P,O-Chelate Ligands and their Reactivity towards $[RuCl_2(PPh_3)_3]$

Robert Gericke, Jörg Wagler

PII: S0277-5387(16)30246-7
DOI: http://dx.doi.org/10.1016/j.poly.2016.06.013
Reference: POLY 12053

To appear in: *Polyhedron*

Received Date: 31 March 2016
Accepted Date: 9 June 2016

Please cite this article as: R. Gericke, J. Wagler, Ruthenium Complexes of Diphenylphosphino Derivatives of Carboxylic Amides: Synthesis and Characterization of bidentate P,N- and P,O-Chelate Ligands and their Reactivity towards $[RuCl_2(PPh_3)_3]$, *Polyhedron* (2016), doi: http://dx.doi.org/10.1016/j.poly.2016.06.013

Ruthenium Complexes of Diphenylphosphino Derivatives of Carboxylic Amides: Synthesis and Characterization of bidentate P,N- and P,O-Chelate Ligands and their Reactivity towards $[RuCl_2(PPh_3)_3]$

*Robert Gericke, Jörg Wagler**

Institut für Anorganische Chemie, Technische Universität Bergakademie Freiberg, D-09596 Freiberg, Germany. E-mail: joerg.wagler@chemie.tu-freiberg.de; Fax: +49 3731 39 4058

Dedicated to Professor Martin A. Bennett on the occasion of his 80th birthday

Key words: Ambidentate Ligands, NMR Spectroscopy, Quantum Chemical Calculations, Ruthenium, Single-Crystal X-Ray Diffraction

Abstract

The carboxylic amides *N*-methylbenzamide (**HLa**), phthalimidine (**HLb**) and pyridine-2-one (**HLc**) were diphenylphosphino-functionalized (with $ClPPh_2$ and a base, *n*-BuLi for **HLa**, triethylamine for **HLb** and **HLc**) to yield the *N*-PPh_2 derivatives of *N*-methylbenzamide (**1a**) and of phthalimidine (**1b**) as well as the *O*-PPh_2 derivative 2-diphenylphosphinoxypyridine (**1c**). Thus, **1a** and **1b** represent P,O-chelate ligands, whereas **1c** is a P,N-chelate ligand. Both P,O-ligands (**1a**, **1b**) react with $[RuCl_2(PPh_3)_3]$ in a two-step fashion to form mono-chelates with *trans*-situated Cl atoms (**2a**, **2b**) upon using a 1:1 stoichiometric ratio or Cl-*trans* bis-chelates ($\mathbf{3a^{II}}$, $\mathbf{3b^{II}}$) upon using two equivalents of the chelator. In contrast, reaction of $[RuCl_2(PPh_3)_3]$ and the P,N-chelator **1c** in 1:1 molar ratio immediately produced a bis-chelate ($\mathbf{3c^{I}}$) with an *all-cis* orientation of the ligands (while 50% of the $[RuCl_2(PPh_3)_3]$ starting material remained unreacted). Compound $\mathbf{3c^{I}}$ slowly isomerizes to the Cl-*trans* isomer ($\mathbf{3c^{II}}$). All isolated

compounds were characterized with multi-nuclear NMR spectroscopy, single-crystal X-ray diffraction and elemental analysis.

1. Introducion

Carboxylic amides [1,2] are well known in coordination chemistry as mono-anionic chelating or bridging ligands. Although N,O-ligands already comprise some hard-soft-ambidenticity, their functionalization with phosphines enlarges the hard-soft variation in the donor set by formation of neutral P,N- or P,O-ligands and generation of 1,4-bidentate ligands capable of forming five-membered chelates. The diversity of products from phosphino-functionalization of carboxylic amides is attributed to the formation of phosphinoamides (*N*-PPh_2 derivatives) and phosphinito-imines (*O*-PPh_2 derivatives) as possible tautomers [3]. (Furthermore, carboxylic amides with phosphine functionalization in α-position [4,5] or other positions of the organic backbone [6], have been studied in transition metal coordination chemistry.) In general, the P,N [7] and P,O [8] bidentate donor sets may exhibit mono- *vs.* bidentate ligand characteristics, and in combination with rather soft transition metal atoms the phosphorus atom represents the superior *σ*-donor over the N or O atom in case of monodentate binding in the transition metal coordination sphere (**A**, **B** and **C** in Scheme 1). This hemilabile property is supportive in many catalytic processes like oligo- and polymerization, carbonylation as well as hydro- and dehydrogenation [8-12]. Moreover, phosphino-functionalized carboxylic amides, which still bear an acidic proton (N–H moiety) can be utilized as mono-anionic bidentate chelators upon deprotonation, and their coordination chemistry has been studied with a variety of transition metal compounds (some examples are shown in Scheme 1, **C**, **D** and **E**) [13,14]. Phosphino-functionalized carboxylic amides devoid of this acidic N–H feature (or in general lacking the capability of forming the corresponding anion) can thus only serve as neutral chelators, hence lacking some electrostatic binding force, which should render these ligands more labile. It is worth noting that literature reports of investigations of the coordination chemistry of this flexible ligand system with ruthenium as one of the most versatile catalytically active transitions metals are very scarce. This served as a motivation for us to investigate the Ru-coordination chemistry of two similar new P,O-ligands (**1a**, **1b**, Scheme 2) and the barely known P,N-ligand **1c** [15,16] starting from their reactions with $[RuCl_2(PPh_3)_3]$.

2. Experimental

2.1. General considerations:

All preparations were carried out under an atmosphere of dry argon using standard Schlenk techniques. Phthalimidine [17] and *N*-methylbenzamide [18] were prepared following literature methods. Tetrahydrofuran (THF) and triethylamine were distilled from sodium/benzophenone and stored under dry argon. Dichloromethane (DCM) was distilled from calcium hydride and stored under argon. Chloroform (stabilized with amylenes) was stored over molecular sieves 3 Å. All other chemicals used were commercially available and used without further purification. Elemental microanalyses (C, H, N) were performed on a 'Vario Micro Cube' analyzer (Elementar, Hanau, Germany).

Yields of the products are reported with respect to the composition found by elemental analyses. Purity of the target compound (ligand or complex) and presence of solvent of crystallization (if applicable) were confirmed by ^{1}H NMR spectroscopy. In some cases, crystals used for single-crystal X-ray diffraction analyses were grown by recrystallization from other solvents. This is pointed out where applicable.

2.2. NMR spectroscopy:

NMR spectra of solutions were recorded on an 'Avance 500' or 'Ascend 400' spectrometer (Bruker Biospin, Rheinstetten, Germany) and internally referenced to tetramethylsilane for ^{1}H and ^{13}C and externally referenced to 85% H_3PO_4 for ^{31}P. Signals were assigned by using ^{1}H,^{1}H-COSY, ^{1}H,^{13}C-HSQC and ^{1}H,^{13}C-HMBC spectroscopy.

2.3. X-ray crystallography:

Single-crystal X-ray diffraction data sets were collected with ω-scans on an 'IPDS-2(T)' diffractometer (STOE, Darmstadt, Germany) using Mo K_α-radiation. The absorption correction was performed with XShape using integration correction type. Structures were solved by direct methods with ShelXS [19] and all non-hydrogen atoms were anisotropically refined in full-matrix least-squares cycles against $|F^2|$ (ShelXL) [20]. Hydrogen atoms were placed in idealized

positions and refined isotropically (riding model). Selected parameters of data collection and refinement of the herein presented structures are listed in the Supporting Information (Tables S20 – S22). In the course of our investigations we determined the crystal structure of phthalimidine (hitherto unknown) and of the new solvate $[RuCl_2(PPh_3)_3]\cdot MeOH$ (see Supporting Information.)

2.4. Computational details:

Optimizations of molecular structures were carried out using the Gaussian09 software [21] at DFT-PBEPBE level with cc-pVTZ for C H N O Cl P atoms and SDD for Ru. NBO analyses were performed using NBO5.G [22] with Gaussian03 [23] at the DFT-B3LYP/6-311+G(d) level for all atoms.

2.5. Synthesis of $[RuCl_2(PPh_3)_3]$

Following literature methods [24, 25], which report the synthesis of $[RuCl_2(PPh_3)_3]$ from commercial $RuCl_3 \cdot 3H_2O$, we prepared $[RuCl_2(PPh_3)_3]$ from elemental Ruthenium without isolating the intermediate Ru(III)-chloride: A mixture of Ruthenium powder (0.750 g, 7.42 mmol), NaOH (4.00 g, 100 mmol) and $NaClO_3$ (2.63 g, 24.7 mmol) was cautiously heated in a crucible (using a Bunsen burner) for 15 min (until the evolution of gas from the deep red melt ceased). The mixture was allowed to cool to ambient temperature and was then dissolved in conc. hydrochloric acid (≈ 250 mL). The acidic solution was evaporated to almost dryness by heating, whereupon further conc. HCl (5 mL) was added and again evaporated by heating (this was repeated three times) before the volatile components were finally evaporated to dryness. The residue was dispensed in MeOH (200 mL) and filtered. The solid residue was washed with MeOH (50 mL). Through the combined filtrate and washings argon was bubbled for 10 min. Subsequently, the mixture was heated under reflux for 10 min, then PPh_3 (12.0 g, 45.8 mmol) was added and the mixture was heated under reflux for 3h. The precipitate was filtered, washed with MeOH (10 mL) and Et_2O (40 mL) and dried *in vacuo* to yield 6.33g (6.61 mmol, 89%) of $[RuCl_2(PPh_3)_3]$. This solvent free compound was used as starting material for the following syntheses.

Prior to the development of the above mentioned protocol, in a test batch a small amount of crude ruthenium chloride was treated with a larger volume of methanolic PPh_3 solution (stirring, reflux). Because of the lower concentration of the reactants, the product did not precipitate as a fine powder but formed some crystals of $[RuCl_2(PPh_3)_3]\cdot MeOH$, which were analyzed by single-crystal X-ray diffraction (see Supporting Information). To the best of our knowledge, this solvate has not been reported in the literature so far.

Also, for $[RuCl_2(PPh_3)_3]$ we obtained additional spectroscopic data which needs to be mentioned here. Whereas Norton et al. [24] reported only one ^{31}P NMR signal (of PPh_3, $\delta = -4$ ppm) for a $CDCl_3$ solution of $[RuCl_2(PPh_3)_3]$, we observed a more complex ^{31}P NMR spectrum of a $CDCl_3$ solution of our product. In addition to the main signal at 41.0 ppm (which was very broad) we observed a signal of PPh_3 and two sets of dublets (both of them characteristic of *cis*-situated Ru-bound PPh_3 groups). We attribute these sets of dublets to two diastereomers of the complex $[(Ph_3P)_2ClRu(\mu\text{-}Cl)_2RuCl(PPh_3)_2]$. This compound has already been characterized crystallographically [26] and in the solid state each Ru atom carries two chemically different PPh_3 ligands *cis* to each other (apical and basal position in a square planar coordination sphere).

$^{31}P\{^1H\}$ NMR ($CDCl_3$, δ ppm): 50.9 (d, J = 28.6 Hz), 47.1 (d, J = 28.6 Hz), 41.0 (br. m, $[RuCl_2(PPh_3)_3]$), 40.6 (d, J = 25.5 Hz), 39.4 (d, J = 25.5 Hz), −5.4 (s, free PPh_3).

*2.6. Syntheses of ligands **1a**, **1b** and **1c***

1a: *N*-Methylbenzamide (1.01 g, 7.50 mmol) was dissolved in THF (20 mL) and cooled with an ice/ethanol mixture (to ca. −10°C). A solution of 2.5M *n*-BuLi in hexanes (3 mL) was added dropwise. The white suspension was stirred with cooling for 1.5 h and subsequently allowed to attain room temperature. Chlorodiphenylphosphine (1.66 g, 7.59 mmol) was added and the clear solution was stirred for 1 h at ambient temperature. The mixture was evaporated to dryness and subsequently suspended in hot $CHCl_3$ (40 mL) for 30 min. After cooling to room temperature the suspension was filtered through Celite. From the filtrate the solvent was removed *in vacuo* and the residue was recrystallized in THF (3 mL). The white crystalline product was suitable for single-crystal X-ray diffraction. The supernatant was decanted and the white solid was dried *in vacuo* to yield 0.529 g (1.66 mmol, 22%) of **1a**.

Anal. Calc. for $C_{20}H_{18}NOP$ (MW: 319.3), requires: C, 75.22; H, 5.68; N, 4.39. Found: C, 75.09; H, 5.75; N, 4.40%. ^{1}H NMR ($CDCl_3$, δ ppm): 2.88 (s, $-CH_3$, 3H), 7.35-7.49 (br. m, aryl, 13H), 7.53 (m, aryl, 2H). $^{13}C\{^{1}H\}$ NMR ($CDCl_3$, δ ppm): 32.6 (d, J = 7.6 Hz), 127.8 (d, J = 6.2 Hz), 128.1 (s), 128.7 (d, J = 5.8 Hz), 129.6 (s), 130.2 (s), 132.0 (d, J = 20.7 Hz), 134.9 (d, J = 16.9 Hz), 136.9 (d, J = 3.2 Hz), 177.0 (d, J = 33.4 Hz). $^{31}P\{^{1}H\}$ NMR ($CDCl_3$, δ ppm): 57.0 (s).

1b: Phthalimidine (1.60 g, 12.0 mmol) was dissolved in THF (80 mL). Triethylamine (1.34 g, 13.2 mmol) was added dropwise and the mixture was stirred for 5 min at ambient temperature. Chlorodiphenylphosphine (2.65 g, 12.0 mmol) was added and the mixture was stirred for three days, whereupon the white precipitate was filtered and washed with THF (2×3 mL). The combined filtrate and washings were evaporated to dryness (condensation of volatiles into a cold trap under reduced pressure) and the residue was recrystallized from THF (27.5 mL). The white crystalline product was suitable for single-crystal X-ray diffraction. The supernatant was decanted, the white solid was washed with Et_2O (3 mL) and dried *in vacuo* to yield 2.33 g (7.34 mmol, 61%) of **1b**.

Anal. Calc. for $C_{20}H_{16}NOP$ (MW: 317.3), requires: C, 75.70; H, 5.08; N, 4.41. Found: C, 75.83; H, 5.18; N, 4.43%. ^{1}H NMR ($CDCl_3$, δ ppm): 4.18 (s, $-CH_2-$, 2H), 7.33 (d, J = 7.54 Hz, aryl, 1H), 7.38-7.50 (br. m, aryl, 11H), 7.54 (dt, J = 7.45 Hz, J =1.10 Hz, aryl, 1H), 7.94 (d, J = 7.54 Hz, aryl, 1H). $^{13}C\{^{1}H\}$ NMR ($CDCl_3$, δ ppm): 49.2 (d, J = 7.1 Hz), 123.0 (s), 124.6 (s), 128.2 (s), 128.7 (d, J = 6.2 Hz), 129.6 (s), 132.1 (s), 132.2 (s), 132.5 (d, J = 21.1 Hz), 135.7 (d, J = 14.4 Hz), 143.8 (s), 173.3 (d, J = 17.3 Hz), $^{31}P\{^{1}H\}$ NMR ($CDCl_3$, δ ppm): 29.7 (s).

1c: This compound was synthesized according to a procedure of Opatz et al. [12] (modified procedure). To a solution of 2-hydroxypyridine (2.00 g, 21.0 mmol) and triethylamine (2.14 g, 21.0 mmol) in THF (30 mL) at 40°C chlorodiphenylphosphine (4.65 g, 21.0 mmol) was added with stirring. The white suspension was stirred at ambient temperature for 1.5 h, then filtered and the white solid was washed with THF (5 mL). The combined filtrate and washings were evaporated to dryness to afford the pure white solid product. Yield: 4.78 g (18.0 mmol, 86%). Crystals suitable for single-crystal X-ray diffraction were obtained by recrystallisation from *n*-hexane. The compound is highly hygroscopic.

Anal. Calc. for $C_{17}H_{14}NOP \cdot 0.7H_2O$ (MW: 291.9), requires: C, 69.95; H, 5.32; N, 4.80. Found: C, 69.68; H, 5.15; N, 4.85%. ^{1}H NMR ($CDCl_3$, δ ppm): 6.91-6.96 (m, aryl, 2H), 7.34-7.41 (m, aryl, 6H), 7.58-7.65 (m, aryl, 5H), 8.19 (m, aryl, 1H). $^{13}C\{^1H\}$ NMR ($CDCl_3$, δ ppm): 112.3 (s, C3, PyO), 118.0 (s, C5, PyO), 128.4 (d, J = 17.2 Hz, *meta*-Ph), 129.6 (s, *para*-Ph), 130.9 (d, J = 23.4 Hz, *ortho*-Ph), 139.1 (s, C4, PyO), 140.7 (d, J = 18.9 Hz, *ipso*-Ph), 147.6 (s, C6, PyO), 162.5 (d, J = 6.9 Hz, C2, PyO). $^{31}P\{^1H\}$ NMR ($CDCl_3$, δ ppm): 100.6 (s).

2.7. Syntheses of Ru-complexes ***2a***, ***2b***, ***3a^{II}***, ***3b^{II}***, ***3c^{I}*** *and* ***3c^{II}***

2a: This compound was synthesized in an analogous manner to **2b** from 128 mg (400 μmol) **1a** and 384 mg (400 μmol) $[RuCl_2(PPh_3)_3]$. The orange crystalline product was obtained in 61% yield (256 mg, 243 μmol). Although the single-crystal used for structure analysis revealed a solvent content of 0.5 Et_2O, elemental analysis indicates that the bulk of the crystalline product consists of $CHCl_3/Et_2O$ solvates of variable solvent site occupancy. Both $CHCl_3$ and Et_2O proton signals were detected in a ^{1}H NMR spectrum of **2a** recorded in CD_2Cl_2.

Anal. Calc. for $C_{56}H_{48}Cl_2NOP_3Ru \cdot 0.2CHCl_3 \cdot 0.3Et_2O$ (MW: 1062.0), requires: C, 64.92; H, 4.86; N, 1.32. Found: C, 64.92; H, 4.83; N, 1.38%. ^{1}H NMR ($CDCl_3$, δ ppm): 2.50 (d, J = 3.72 Hz, -CH_3, 3H), 6.74-6.85 (br. m, *meta*-PPh_3, 12H), 6.89 (d, J = 7.50 Hz, *ortho*-(MeNCOPh), 2H), 7.02 (m, *ortho*-PPh_3, 6H), 7.08 (m, *para*-PPh_3, 3H), 7.11-7.21 (m, *para*-PPh_3, *ortho*-PPh_3, 9H), 7.24-7.31 (m, *meta*-(MeNCOPh), *meta*-Ph_2P(MeNCO), 6H), 7.37 (t, J = 7.46 Hz, *para*-(MeNCOPh), 1H), 7.40-7.47 (m, *ortho*-Ph_2P(MeNCO), *para*-Ph_2P(MeNCO), 6H). $^{13}C\{^1H\}$ NMR ($CDCl_3$, δ ppm): 35.6 (s, -CH_3), 126.4 (d, J = 8.3 Hz, *meta*-PPh_3), 126.9 (s, *ortho*-(MeNCOPh)), 127.0 (d, J = 9.2 Hz, *meta*-PPh_3), 127.4 (d, J = 8.8 Hz, *meta*-Ph_2P(MeNCO)), 127.9 (s, *meta*-(MeNCOPh)), 128.5 (s, *para*-PPh_3), 128.8 (s, *para*-PPh_3), 129.5 (m, *ipso*-Ph_2P(MeNCO)), 129.8 (s, *para*-(MeNCOPh)), 130.1 (s, *para*-Ph_2P(MeNCO)), 132.5 (d, J = 34.3 Hz, *ipso*-PPh_3), 133.9 (s, *ipso*-(MeNCOPh)), 134.1 (d, J = 9.7 Hz, *ortho*-Ph_2P(MeNCO)), 134.9 (d, J = 9.4 Hz, *ortho*-PPh_3), 136.2 (d, J = 8.0 Hz, *ortho*-PPh_3), 136.4 (d, J = 44.0 Hz, *ipso*-PPh_3), 183.2 (d, J = 13.8 Hz, NCO). $^{31}P\{^1H\}$ NMR ($CDCl_3$, δ ppm): 108.2 (dd, J = 342 Hz, J = 29 Hz, Ph_2P(MeNCOPh), 1P), 41.4 (t, J = 29 Hz, PPh_3, 1P), 19.0 (dd, J = 342 Hz, J = 29 Hz, PPh_3, 1P).

2b: **1b** (145 mg, 457 μmol) and $[RuCl_2(PPh_3)_3]$ (438 mg, 457 μmol) were dissolved in $CHCl_3$ (5 mL). The deep red solution was stirred for 3 h and then stored undisturbed at room temperature.

After one week, red crystals, suitable for single-crystal X-ray diffraction, were obtained by vapor diffusion of Et_2O into the reaction mixture. The supernatant was removed by decantation and the solid was washed with Et_2O (3 mL) and dried *in vacuo.* Yield: 355 mg (307 µmol, 67%). The product exhibits poor solubility in various organic solvents. Whereas singe-crystal X-ray diffraction analysis confirms a higher solvent content of the crystal used, the average content of solvent of crystallization of the product was found to be lower (by elemental analysis).

Anal. Calc. for $C_{56}H_{46}Cl_2NOP_3Ru \cdot 1.2CHCl_3$ (MW: 1157.1), requires: C, 59.37; H, 4.11; N, 1.21. Found: C, 59.51; H, 4.05; N, 1.25%. $^{31}P\{^1H\}$ NMR (CD_2Cl_2, δ ppm): 84.2 (dd, J = 31 Hz, J = 344 Hz, Ph_2P(phthal.), 1P), 41.7 (t, J = 31 Hz, PPh_3, 1P), 20.8 (dd, J = 31 Hz, J = 344 Hz, PPh_3, 1P), compound shows loss of PPh_3 in solution: 110.8 (d, J = 37 Hz, Ph_2P(phthal.), 0.1P), 52.2 (d, J = 37 Hz, PPh_3, 0.1P), −5.6 (s, PPh_3, 0.1P).

3a^{II}: This compound was synthesized in an analogous manner to **3b^{II}** from 100 mg (313 µmol) **1a** and 150 mg (156 µmol) [$RuCl_2(PPh_3)_3$]. The compound was obtained as an orange crystalline solid by vapor diffusion of Et_2O into a $CHCl_3$ solution, followed by decantation and drying *in vacuo*. As this solid was a very fine powder and contained some impurities (according to ^1H NMR), the crude product was dissolved in CH_2Cl_2 (2 mL) and crystallized by vapor diffusion of Et_2O, followed by decantation and drying *in vacuo*. Yield: 52 mg (61 µmol, 39%). In addition to solvent free crystals (see single-crystal structure analysis of **3a^{II}**, crystals obtained from this preparation), elemental analysis indicates that the bulk of the crystalline product also consists of CH_2Cl_2 solvates.

Anal. Calc. for $C_{40}H_{36}Cl_2N_2O_2P_2Ru \cdot 0.4CH_2Cl_2$ (MW: 844.6), requires: C, 57.45; H, 4.39; N, 3.32. Found: C, 57.48; H, 4.22; N, 3.15%. ^1H NMR ($CDCl_3$, δ ppm): 3.04 (m, -CH_3, 6H), 7.22 (m, *meta*-Ph_2P, 8H), 7.37-7.48 (br. m, aryl, 10H), 7.54 (m, aryl, 8H), 7.70 (m, aryl, 4H). $^{13}C\{^1H\}$ NMR ($CDCl_3$, δ ppm): 36.9 (s, -CH_3), 127.5 (m, *meta*-Ph_2P), 128.1 (s, aryl, (MeNCOPh)), 128.2 (s, aryl, (MeNCOPh)), 130.5 (s, *para*-Ph_2P), 130.7 (s, *para*-(MeNCOPh)), 131.1 (br. m, *ipso*-Ph_2P), 134.0 (m, *ipso*-(MeNCOPh)), 134.6 (m, *ortho*-Ph_2P), 183.0 (m, NCO). $^{31}P\{^1H\}$ NMR ($CDCl_3$, δ ppm): 135.6 (s).

3b^{II}: **1b** (200 mg, 630 µmol) and [$RuCl_2(PPh_3)_3$] (302 mg, 315 µmol) were dissolved in $CHCl_3$ (2 mL). The red solution was stirred for 5 min and subsequently stored at room temperature. After one day, orange crystals, suitable for single-crystal X-ray diffraction, were formed. The supernatant was removed by decantation and the solid was washed with Et_2O (2 mL) and dried *in vacuo*. Yield: 137 mg (138 µmol, 44%). From this crystalline product a crystal structure of the solvate **3b^{II}**·7 $CHCl_3$ was determined, the solvent was heavily disordered and had to be treated with SQUEEZE (see Supporting Information). As indicated by elemental analysis, the bulk of this crystalline product has lower $CHCl_3$ content. Crystals of better quality for single-crystal X-ray diffraction were obtained by vapor diffusion of Et_2O into a CH_2Cl_2 solution of **3b^{II}**.

Anal. Calc. for $C_{40}H_{32}Cl_2N_2O_2P_2Ru \cdot 1.55CHCl_3$ (MW: 991.7), requires: C, 50.32; H, 3.41; N, 2.82. Found: C, 50.28; H, 3.51; N, 2.65%. ^{1}H NMR (CD_2Cl_2, δ ppm): 4.61 (s, -CH_2-, 4H), 7.20 (dd, *J* = 7.37 Hz, *J* = 7.94 Hz, *meta*-Ph, 8H), 7.39 (m, *ortho*-Ph, 4H), 7.42 (t, *J* = 7.37 Hz, *para*-Ph, 8H), 7.48 (d, *J* = 7.49 Hz, -H4 (phthal.), 2H), 7.61 (dd, *J* = 7.58 Hz, *J* = 7.99 Hz, -H6 (phthal.), 2H), 7.66 (ddd, *J* = 1.30 Hz, *J* = 7.49 Hz, *J* = 7.99 Hz, -H5 (phthal.), 2H), 8.25 (d, *J* = 7.58 Hz, -H7 (phthal.), 2H). ^{13}C{^{1}H} NMR (CD_2Cl_2, δ ppm): 48.8 (s, C3 (phthal.)), 124.1 (s, C4 (phthal.)), 125.5 (s, C7 (phthal.)), 127.7 (m, *meta*-Ph), 129.1 (s, C6 (phthal.)), 129.5 (m, C7a (phthal.)), 131.3 (s, *para*-Ph), 132.3 (br. m, *ipso*-Ph), 133.6 (s, C5 (phthal.)), 135.0 (m, *ortho*-Ph), 147.6 (s, C3a (phthal.)), 182.2 (m, C1 (phthal.)). ^{31}P{^{1}H} NMR (CD_2Cl_2, δ ppm): 118.6 (s).

3c^{I}: **1c** (116 mg, 415 µmol) and [$RuCl_2(PPh_3)_3$] (200 mg, 209 µmol) were dissolved in THF (3 mL). The deep red solution was heated under reflux for 10 min, whereupon the yellow suspension was filtered. The yellow solid was washed with THF (2 mL) and dried *in vacuo*. Yield: 45 mg (60 µmol, 29%). Elemental analysis and ^{1}H NMR spectroscopy confirm the solvent content of this product. Crystals of a $CHCl_3$ solvate, suitable for single-crystal X-ray diffraction were obtained by vapor diffusion of pentane into a $CHCl_3$ solution of **3c^{I}**.

Anal. Calc. for $C_{34}H_{28}Cl_2N_2O_2P_2Ru \cdot 0.3THF$ (MW: 752.2) requires: C, 56.21; H, 4.07; N, 3.72. Found: C, 56.17; H, 4.07; N, 3.68%. ^{1}H NMR ($CDCl_3$, δ ppm): 6.36 (ddd, *J* = 1.31 Hz, *J* = 5.96 Hz, *J* = 7.31Hz, -H5 (PyO-2), 1H), 6.71 (m, PPh, 2H), 6.93-7.04 (br. m, -H3 (PyO-2), -H6 (PyO-2), PPh, 6H), 7.09-7.19 (br. m, PPh, 4H), 7.27-7.40 (br. m, -H3 (PyO-1), -H5 (PyO-1), -H4 (PyO-2), PPh, 7H), 7.56-7.64 (br. m, PPh, 4H), 7.89 (m, -H4 (PyO-1), 1H), 8.24 (m, PPh, 2H),

9.89 (m, -H6 (PyO-1), 1H). $^{13}C\{^{1}H\}$ NMR ($CDCl_3$, δ ppm): 111.1 (m, 2x C3 (PyO)), 118.3 (s, C5 (PyO-2)), 119.7 (d, J = 2.0 Hz, C5 (PyO-1)), 127.6 (d, J = 10.4 Hz, PPh), 127.7 (d, J = 10.9 Hz, PPh), 127.8 (d, J = 9.7 Hz, PPh), 128.1 (d, J = 10.7 Hz, PPh), 128.5 (d, J = 12.5 Hz, PPh), 129.1 (d, J = 11.2 Hz, PPh), 129.8 (d, J = 2.0 Hz, *para*-PPh), 129.9 (d, J = 2.1 Hz, *para*-PPh), 130.5 (d, J = 2.1 Hz, *para*-PPh), 131.0 (d, J = 1.6 Hz, *para*-PPh), 131.2 (d, J = 12.4 Hz, PPh), 133.3 (d, J = 11.6 Hz, PPh), 133.9 (d, J = 49.1 Hz, *ipso*-PPh), 134.3 (d, J = 49.2 Hz, *ipso*-PPh), 137.2 (d, J = 47.5 Hz, *ipso*-PPh), 138.4 (s, C4 (PyO-2)), 140.8 (s, C4 (PyO-1)), 140.9 (dd, J = 4.0 Hz, J = 52.6 Hz, *ipso*-PPh), 150.1 (s, C6 (PyO-2)), 150.2 (s, C6 (PyO-1)), 163.1 (m, C2 (PyO)), 165.0 (m, C2 (PyO)). $^{31}P\{^{1}H\}$ NMR ($CDCl_3$, δ ppm): 173.3 (d, J = 35.2 Hz, 2P), 172.5 (d, J = 35.2 Hz, 1P).

3c^{II}: Compound **3c^{II}** was synthesized by isomerization of **3c^{I}** (80 mg, 110 μmol) in $CHCl_3$ (1 mL) solution. After stirring for 6 weeks at room temperature the suspension was filtered, the yellow solid was washed with $CHCl_3$ (0.5 mL) and dried *in vacuo*. Yield: 19 mg (26 μmol, 24%). Crystals of a CH_2Cl_2 solvate, suitable for single-crystal X-ray diffraction analysis, were grown by vapor diffusion of Et_2O into a CH_2Cl_2 solution of **3c^{II}**.

Anal. Calc. for $C_{34}H_{28}Cl_2N_2O_2P_2Ru$ (MW: 730.5), requires: C, 55.90; H, 3.86; N, 3.83. Found: C, 55.47; H, 3.98; N, 3.76%.

^{1}H NMR ($CDCl_3$, δ ppm): 7.15 (m, -H5 (PyO), 2H), 7.21 (m, *meta*-PPh_2, 8H), 7.33 (br. m, *para*-PPh_2, -H3 (PyO), 6H), 7.41 (m, *ortho*-PPh_2, 6H), 7.77 (m, -H4 (PyO), 2H), 8.57 (m, -H6 (PyO), 2H). $^{13}C\{^{1}H\}$ NMR ($CDCl_3$, δ ppm): 112.2 (s, C3), 119.2 (s, C5), 127,5 (m, *meta*-PPh_2), 130.6 (s, *para*-PPh_2), 132.3 (m, *ortho*-PPh_2), 136.7 (br. m, *ipso*-PPh_2), 140.2 (s, C4), 149.7 (s, C6), 163.8 (s, C2). $^{31}P\{^{1}H\}$ NMR ($CDCl_3$, δ ppm): 178.5 (s).

3. Results and Discussion

3.1. Chelating ligands

Reaction of the lithium salt of *N*-methylbenzamide (**HLa**) with chlorodiphenylphosphine afforded the *N*-PPh_2 derivative **1a** (Scheme 2). Whereas in this case the lithium salt route proved

to be more efficient than the kinetically hampered reaction of *N*-methylbenzamide and triethylamine as a supporting base (we attribute this to the lower acidity of **HLa**), **1b** and **1c** were accessible by reaction of phthalimidine (**HLb**) or 2-hydroxypyridine (**HLc**) with chlorodiphenylphosphine and triethylamine (Et_3N). According to their ^{31}P NMR shifts (**1a**: 57.0 ppm, **1b**: 29.7 ppm), both compounds feature a P–N bond, as these ^{31}P NMR shifts are in good agreement with related *N*-PPh_2 substituted compounds such as Ph_2P-NH(COMe) (21.6 ppm) or Ph_2P-NMe(COMe) (55.1 ppm) [27]. The dublet splitting of $^{13}C\{^1H\}$ NMR signals of the carbon atoms in direct contiguity of the N atoms, caused by $^2J_{P,C}$ coupling, underpins the formation of phosphinoamides in both cases. The presence of only one set of NMR signals allows for the conclusion that one of the tautomers was formed exclusively. Finally, single-crystal X-ray diffraction analysis confirms the P–N bonding situation and, furthermore, reveals two interesting differences between the molecular conformations of **1a** and **1b**. For the P-N-C-O sequence a zigzag arrangement is found in **1a** and a U-shape in **1b**, the latter leads to a weakly capped coordination sphere around the phosphorus atom in **1b** with a P···O separation of 3.011(1) Å (Fig. 1). Also, the P–N bond in **1b** is significantly shorter than in **1a** (Table 1). This is in accord with the lower steric demand of the phthalimidine anion because of the N atom being incorporated in a five-membered ring and it could also be a result of electrostatic bond strengthening. As to the latter, calculations of the Natural Charges (NCs) reveal a marginally more negative sum of NCs at phthalimidyl in comparison to the *N*-methylbenzamidyl fragment (–0.472 *vs.* –0.460, respectively). The combination of these characteristics (*O*-capped phosphorus coordination sphere, higher ionicity of the P–N bond, shorter P–N bond) may contribute to the noticeable upfield shift of the ^{31}P NMR signal of **1b** relative to **1a** ($\Delta(\delta) = -27.3$ ppm).

In contrast to **1a** and **1b**, compound **1c** features a P–O bond. This is evident from a characteristic downfield shift of the ^{31}P NMR signal, which emerges around 100 ppm and is characteristic of a Ph_2P-O-aryl moiety (like in Ph_2P-O-*p*-C_6H_4-O-PPh_2, $\delta^{31}P = 110.5$ ppm) [28]. Also, only for one carbon atom (C1) $^2J_{P,C}$ coupling is observed, and the single-crystal X-ray structure (Fig. 1) proves the identity of this compound. Retention of the aromatic character of the pyridine moiety in **1c** may play a role as a driving force for *O*-functionalization in this particular case.

3.2. Ruthenium(II) mono-chelates

Reaction of the coordinatively unsaturated complex $[RuCl_2(PPh_3)_3]$ with one equivalent of **1a** or **1b** yields the expected mono-chelate compounds **2a** and **2b**, respectively, accompanied by liberation of one equivalent of triphenylphosphine (Scheme 3). The Ru coordination spheres in these compounds are slightly distorted octahedral with *trans*-situated Cl atoms (Fig. 2). The Cl-Ru-Cl axis is significantly off linearity with the Cl atoms bent towards the P,O-chelate ligand (Table 2). We attribute this distortion to the greater steric demand of the *cis*-situated PPh_3 ligands on the opposite side. Nonetheless, with respect to the starting material $[RuCl_2(PPh_3)_3]$ (Cl-Ru-Cl angles reported: 155.99(3)° [this paper], 157.2(2)°, 159.24(4)°, 159.83(3)°, 162.53(3)° [29-32]), the Cl1-Ru1-Cl2 angles in **2a** and **2b** are widened. In **2a** and **2b** the Ru1–P3 bond to one of the triphenylphosphine ligands is significantly longer than the other Ru–P bonds. Whereas P2 (also from a triphenylphosphine) is *trans* to a rather weak donor (the O atom of the chelate ligand) and thus forms a short Ru–P bond, the chelate P atom P1 is *trans*-disposed to P3 and, due to its lower steric demand and chelate effect, forming a shorter Ru–P bond at the expense of Ru1–P3 bond strength, thus resulting in a bond length difference of about 0.19 Å (**2a**) or 0.14 Å (**2b**) between the two Ru–PPh_3 bonds within one molecule. This characteristic is known from a complex with similar Ru coordination sphere, i.e., $[RuCl_2(P\text{-}Ph_2P\text{-}CH_2COOEt)_2(\kappa P,O\text{-}Ph_2P\text{-}CH_2COOEt)]$ with *trans*-disposed Ru–Cl bonds, a P,O-chelate and two monodentate phosphane ligands [33]. This compound exhibits a difference of 0.14 Å between the two Ru–$PPh_2(CH_2COOEt)$ bonds, the longer being *trans* to the chelate P, the shorter being *trans* to the chelate O atom. The chelate bonds Ru1–P1 and Ru1–O1 in compound **2b** are significantly longer than the corresponding bonds in **2a**. Furthermore, there are differences in the angles between the O-C- and N-P-axes (59.8(1)° in **2a**, 61.9(2)° in **2b**) and the angle formed between the idealized pyramidal axis of the C_2NP pyramid and the Ru–P bond (18.5° in **2a**, 19.1° in **2b**). This allows for the conclusion that steric constraints of the phthalimidine moiety pose a hindrance for the optimization of Ru–O and Ru–P orbital interactions and the pronounced distance of the Ru atom from the chelate in **2b** serves the purpose of optimizing Ru-P orbital interactions. Whereas the P1–N1 bond in **2a** and **2b** is similar to the corresponding bond in the free ligand **1a** and **1b**, respectively, Ru-complexation causes bond length changes within the carboxylic moiety. In both complexes a significantly longer (by 0.02 Å) C=O and shorter (by 0.02 Å) C–N bond is observed.

Incorporation of ligands **1a** and **1b** in Ru complexes **2a** and **2b**, respectively, causes a downfield shift of the ^{31}P resonance by about 50 ppm. The difference between both ^{31}P NMR shifts (which is 27.3 ppm between **1a** and **1b**) is in general retained for **2a** and **2b** ($\Delta(\delta)$ = 24.0 ppm). In the $^{31}P\{^1H\}$ NMR spectrum compounds **2a** and **2b** show the expected coupling pattern of an ABX spin system, with a characteristic *trans* $^2J_{P,C}$ coupling around 340 Hz and *cis* $^2J_{P,C}$ coupling around 30 Hz. As already indicated by the long Ru1–P3 bond in the crystal structures of **2a** and **2b**, in solution both complexes exhibit the tendency to split off a PPh_3 molecule (an effect which is also observed for $[RuCl_2(PPh_3)_3]$, see experimental section). An extra set of signals in 1:1:1 ratio (of lower intensity) emerges in the $^{31}P\{^1H\}$ NMR spectrum of **2b**, one of the signals representing PPh_3 (–5.6 ppm), whereas the other two signals (dublets at 110.8 and 52.2 ppm, $^2J_{P,C}$ = 37 Hz) are representative of *cis*-situated PPh_3 and $NPPh_2$ ligands. (In case of **2a**, a greater variety of low intensity signals emerges in addition to a signal of PPh_3).

3.3. Ruthenium(II) bis-chelates

The reaction of $[RuCl_2(PPh_3)_3]$ with two equivalents of **1a** or **1b** leads to the formation of the Cl-*trans* isomers $\mathbf{3a^{II}}$ and $\mathbf{3b^{II}}$, respectively (Scheme 3). In addition to the characteristic signals of PPh_3, **1a** (or **1b**), **2a** (or **2b**) and $\mathbf{3a^{II}}$ (or $\mathbf{3b^{II}}$) in both cases $^{31}P\{^1H\}$ NMR spectra of the crude reaction mixture exhibit an extra set of dublet signals characteristic of *cis*-arranged chemically non-equivalent $NPPh_2$ moieties (with ligand **1a**: 137.4, 129.3 ppm, $^2J_{P,C}$ = 34.1 Hz; with ligand **1b**: 122.0, 107.2 ppm, $^2J_{P,C}$ = 37.2 Hz). These extra signals and the characteristic signals of **1a** (or **1b**), **2a** (or **2b**) decrease in favor of the singlet signal of $\mathbf{3a^{II}}$ (or $\mathbf{3b^{II}}$). This hints at the formation of the *all-cis* isomers $\mathbf{3a^{I}}$ and $\mathbf{3b^{I}}$ as intermediates (Scheme 3).

In sharp contrast to the formation of **2a** and **2b**, the reaction of $[RuCl_2(PPh_3)_3]$ with one equivalent of **1c** leads to the formation of the *all-cis* isomer of bis-chelate compound **3c** ($\mathbf{3c^{I}}$) in addition to unreacted starting material $[RuCl_2(PPh_3)_3]$ (Scheme 3). Compound $\mathbf{3c^{I}}$ is also accessible along a deliberate synthesis route by using two equivalents of **1c**. In solution the *all-cis* isomer $\mathbf{3c^{I}}$ slowly isomerizes to the Cl-*trans* isomer $\mathbf{3c^{II}}$. Monitoring of the crude reaction mixture by $^{31}P\{^1H\}$ NMR spectroscopy revealed that this isomerization does not go to completion within three months. The isolation of pure Cl-*trans* isomer $\mathbf{3c^{II}}$ was possible by crystallization from chloroform, in which the *all-cis* isomer $\mathbf{3c^{I}}$ remains in solution.

We succeeded in crystallizing (and determining the crystal structures of) all three *trans*-Cl isomers **3a^{II}**, **3b^{II}** and **3c^{II}** as well as of the *all-cis* isomer **3c^{I}** (Fig. 2 and Fig. 3). The Ru–P bonds in **3a^{II}** and **3b^{II}** are significantly shorter than the corresponding bonds in **2a** and **2b**, caused by reduction of steric demand upon replacing the former two PPh_3 ligands by another P,O-chelator. As a result of the incorporation of the two *cis*-disposed P atoms in chelating ligands significant widening of the P1-Ru1-P2 angles is observed. In spite of the overall reduced steric pressure in the Ru coordination sphere, the *cis* arrangement of the two PPh_2 groups still causes notable bending of the Cl1-Ru1-Cl2 axis away from the aryl groups. Unexpectedly, in **3a^{II}** the Ru1–Cl1 bond (2.368(1) Å) is around 0.04 Å shorter than the *trans*-disposed Ru1–Cl2 bond (2.409(1) Å), whereas in compounds **2a**, **2b** and **3b^{II}** the Ru–Cl bond lengths are found within a very narrow range (2.404(1) – 2.424(1) Å). Analysis of the molecular packing revealed a special environment for atom Cl1 in **3a^{II}**: a methyl group from a neighboring molecule poses a steric hindrance and prevents the formation of multiple attractive aryl-C-H···Cl contacts with this chlorine atom (only one of these contacts is found for Cl1 in **3a^{II}**, whereas the other Cl atoms are involved in multiple contacts of this kind).

In the structurally related Cl-*trans* isomer **3c^{II}**, the Ru–Cl bond lengths (Table 3) are in the same range as mentioned above. The different *trans*-donor situation in **3c^{I}**, however, causes notable Ru–Cl bond lengthening (for the three crystallographically independent molecules in the crystal structure of **3c^{I}** Ru–Cl bonds are found in the range 2.42-2.48 Å), with the longer Ru–Cl bond found *trans* to Ru–P, the shorter one *trans* to Ru–N. Even more pronounced bond lengthening is found for the Ru–N bond *trans* to P, whereas the other Ru–N bond (*trans* to Ru–Cl) is about 0.1 Å shorter.

Interestingly, the three different P,N/O-ligands **1a**, **1b** and **1c** show similar isomerization behavior with respect to the five possible isomers of Ruthenium bis-chelates shown in Scheme 4. The relative energies of the isomers **3^{I}**-**3^{V}** obtained by calculations at DFT-PBEPBE level (Table 4) are in accord with the experimental observations. That is, with the P,O-chelators isomer **3^{II}** (which has been isolated and characterized) is predicted as the thermodynamically stable isomer. The proposed intermediate isomer **3^{I}** was predicted to be the second stable isomer (+7 and +5 kcal/mol higher in energy for **3a** and **3b**, respectively). With the P,N-chelating ligand **1c** isomers

3$^{\mathbf{I}}$, **3**$^{\mathbf{II}}$ and **3**$^{\mathbf{V}}$ are predicted to be very similar in energy (0.0, 2.4, 2.3 kcal/mol, respectively). Thus, it is not surprising that we were able to isolate two of these isomers (**3c**$^{\mathbf{I}}$ and **3c**$^{\mathbf{II}}$). Whereas Langer et al. [12] reported these three isomers with a similar P,N-bidentate ligand, in our study of the coordination behavior of **1c** towards Ru(II) we found the initial formation of **3c**$^{\mathbf{I}}$ (as a kinetic product) which slowly isomerizes into a mixture of **3c**$^{\mathbf{I}}$ and **3c**$^{\mathbf{II}}$, where **3c**$^{\mathbf{II}}$ could be separated by crystallization. There were no spectroscopic hints at the formation of the N-*trans* isomer **3**$^{\mathbf{V}}$.

4. Conclusions

Two new P,O-chelating ligands (**1a** and **1b**) and one P,N-chelating ligand (**1c**) were synthesized and there coordination behavior towards Ru(II) was explored. As these carboxylic amide derived phosphanes lack acidic N–H or O–H bonds in their carboxylic amide motif, they act as non-ionic ligands. In all cases we observed chelation of the Ru atom by these ligands with liberation of initially Ru-bound PPh_3 ligands. Whereas the P,O-ligands **1a** and **1b** were able to replace one or all three PPh_3 ligands from $[RuCl_2(PPh_3)_3]$, forming mono- or bis-chelate complexes, respectively, in a step-wise manner, the P,N-ligand **1c** afforded bis-chelate complexes. Whereas Cl-*trans* configuration was encountered with all three bis-chelated Ru complexes obtained from **1a**, **1b** and **1c**, and quantum chemical analyses proved these compounds to be the thermodynamically favored isomers for the combinations $[RuCl_2(\kappa^2P,O\text{-}\mathbf{1a})_2]$ and $[RuCl_2(\kappa^2P,O\text{-}\mathbf{1b})_2]$, we observed ^{31}P NMR spectroscopic data which are consistent with the initial formation of the *all-cis* isomers as kinetically driven intermediates. For $[RuCl_2(\kappa^2P,N\text{-}\mathbf{1c})_2]$ we succeeded in isolating both isomers (Cl-*trans* and *all-cis*) as crystalline solids. Even though these isomers are similar in energy (according to computational analyses), slow isomerization of *all-cis* into Cl-*trans* (observed by time dependent NMR spectroscopy) proved the Cl-*trans* isomer the favored species in this system as well. Neither in the sterically more crowded mono-chelates $[RuCl_2(PPh_3)_2(\kappa^2\text{-}\mathbf{1})]$ nor in the bis-chelates $[RuCl_2(\kappa^2\text{-}\mathbf{1})_2]$ hemi-labile behavior of the O- or N-donor site was observed. Instead, for the mono-chelates dissociation of PPh_3 was observed in solution, and for the bis-chelates solution NMR spectra are in accord with retention of the Cl-*trans* octahedral Ru-coordination sphere.

Schemes:

Scheme 1. Examples of Ru-complexes with hemi-labile P,N- (A) and P,O-chelating ligands (B, C) as well as transition metal complexes with mono-anionic chelating ligands upon carbamide deprotonation (C, D, E).

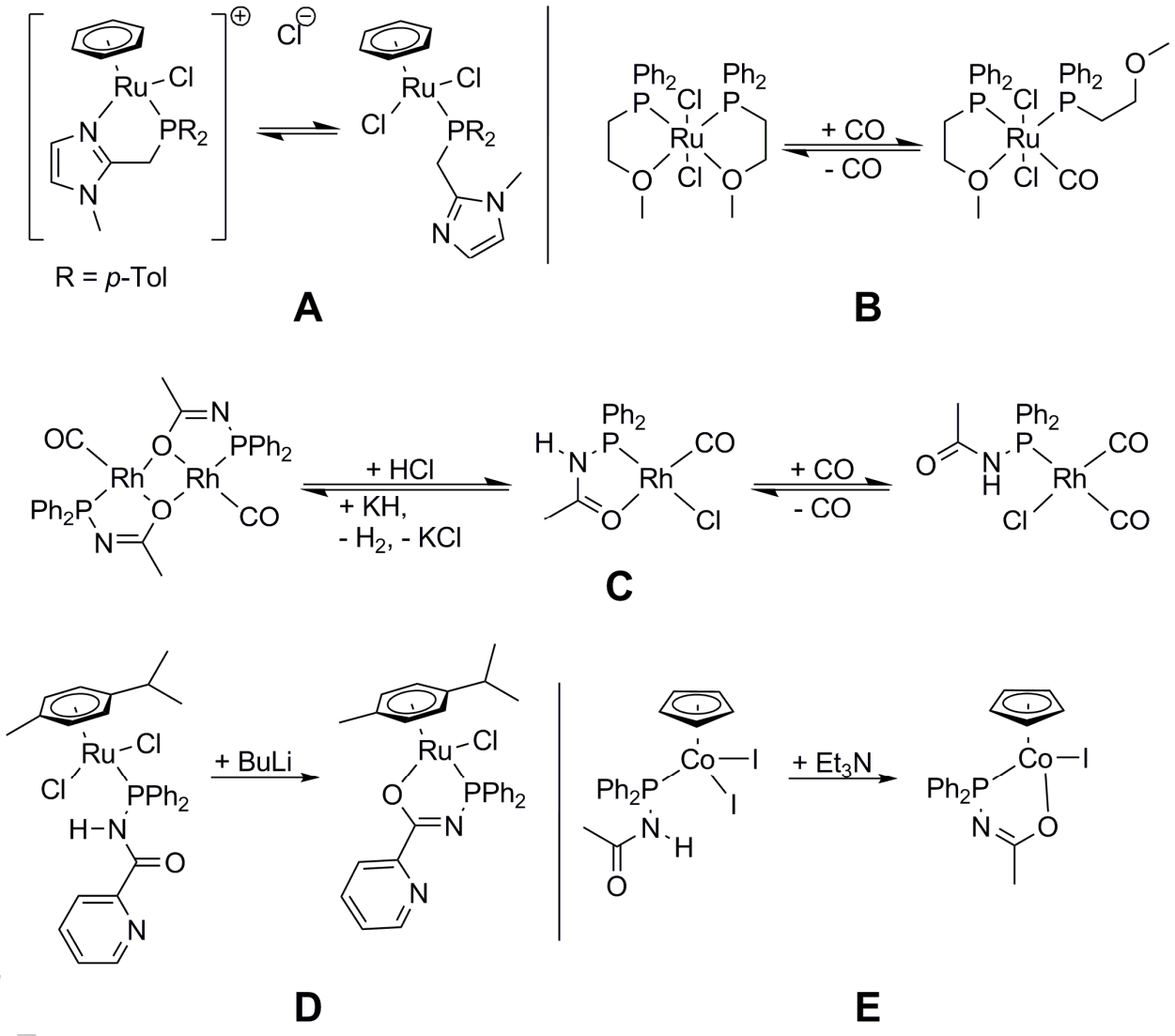

Scheme 2. Synthesis of compounds 1a-c.

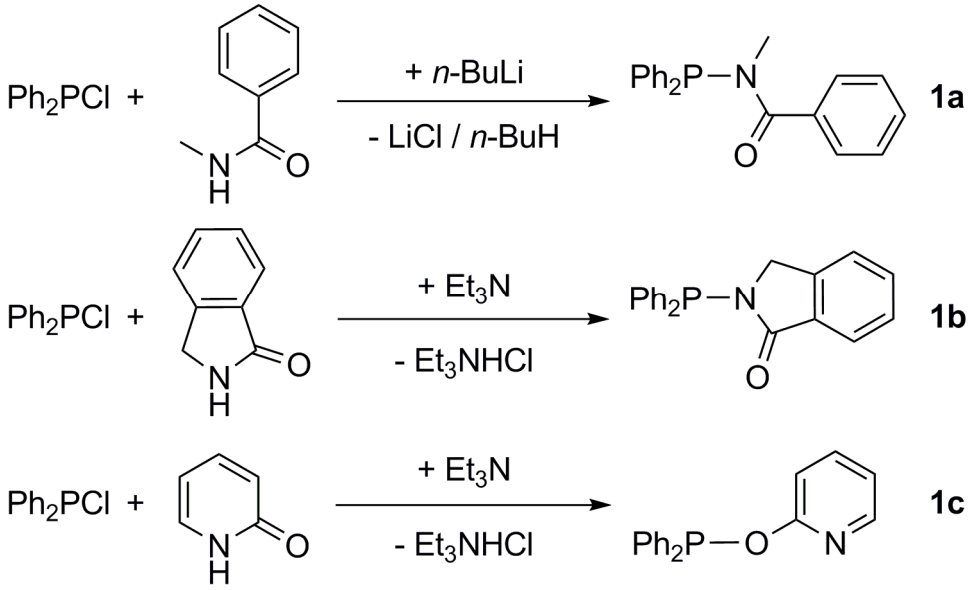

Scheme 3. Synthesis of compounds 2a,b and 3a^{I}-c^{II} (E = N,O).

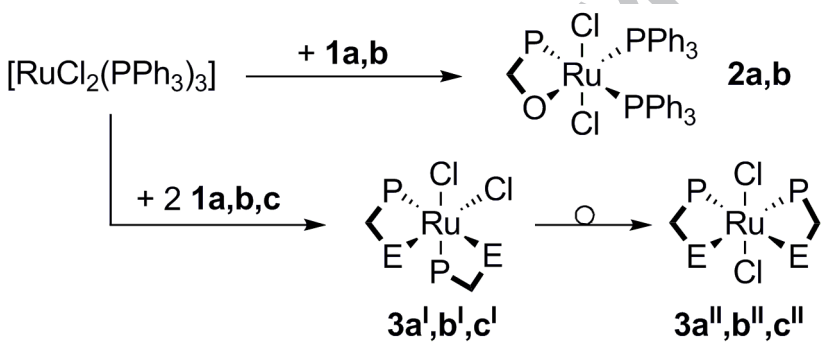

Scheme 4. Isomers of Ruthenium bis-chelates [$RuCl_2(L)_2$] for the herein reported ligands L = 1a, 1b and 1c, (E = N,O).

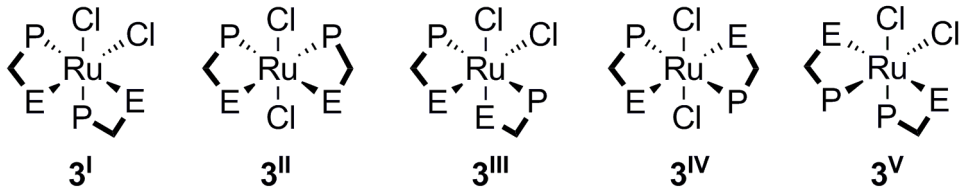

Figures:

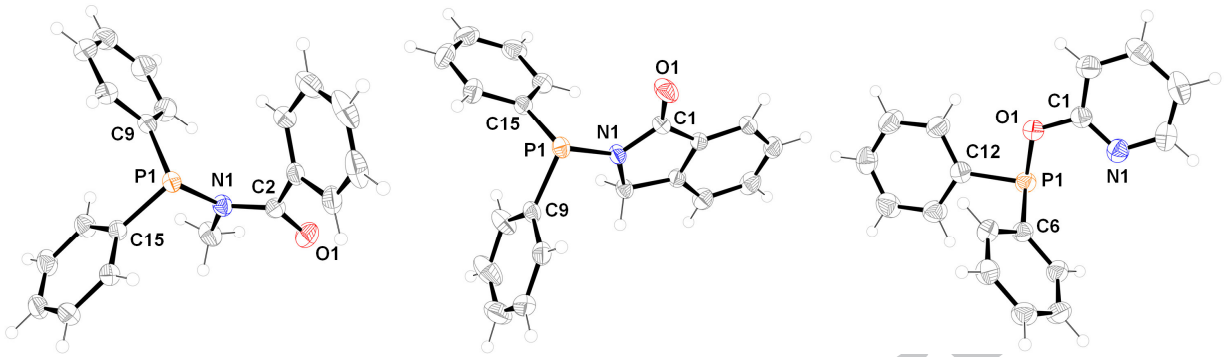

Fig. 1. ORTEP drawing of (from left to right) compound **1a**, **1b** and **1c**. Thermal displacement ellipsoids are displayed at the 50% probability level.

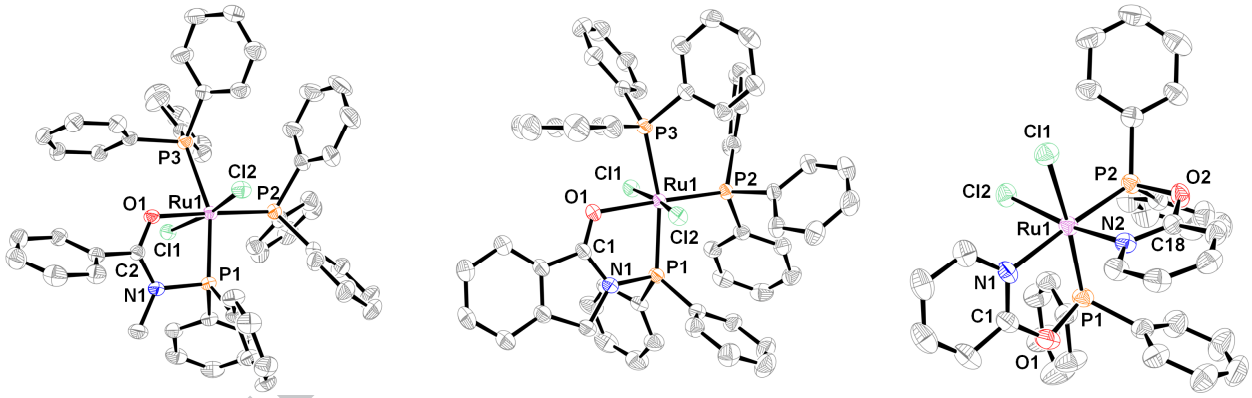

Fig. 2. ORTEP drawing of (from left to right) compounds **2a**, **2b** and **3c**$^{\mathbf{I}}$. Thermal displacement ellipsoids are displayed at the 50% probability level. H atoms and solvent molecules are omitted for more clarity. For **3c**$^{\mathbf{I}}$ only one of the three crystallographically independent (but conformationally identical) molecules is depicted.

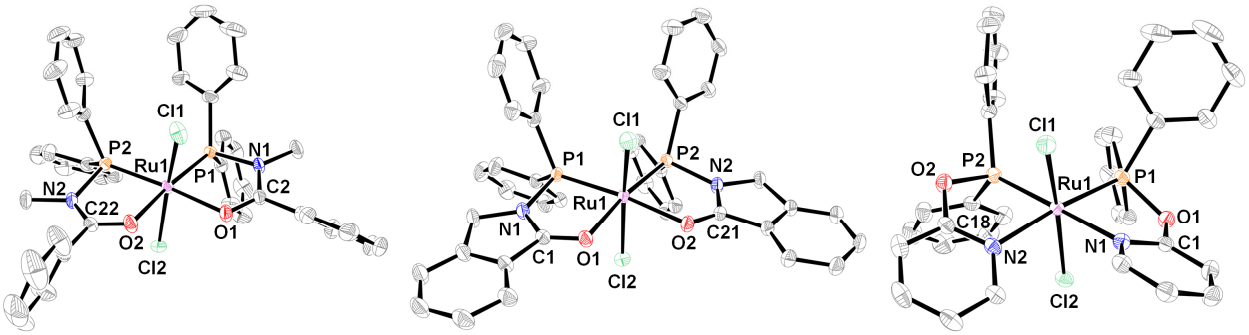

Fig. 3. ORTEP drawing of (from left to right) compound **3a**$^{\mathbf{II}}$, **3b**$^{\mathbf{II}}$ and **3c**$^{\mathbf{II}}$. Thermal displacement ellipsoids are displayed at the 50% probability level. H atoms and solvent molecules are omitted for clarity.

Tables:

Table 1

Selected bond lengths (Å) and angles (°) of **1a**, **1b** and **1c**.

	1a	**1b**	**1c**
P-N/O	1.7504(9)	1.7276(11)	1.6839(14)
P-C	1.8295(11)	1.8250(14)	1.825(2)
	1.8376(10)	1.8263(14)	1.829(2)
$C_{carbonyl}$-N	1.3802(14)	1.3849(16)	1.322(3)
$C_{carbonyl}$-O	1.2269(13)	1.2197(17)	1.362(2)
C-P-C	100.28(5)	102.57(6)	100.67(9)
C-P- N/O	101.39(4)	98.81(6)	95.21(8)
	103.17(5)	102.45(6)	100.95(8)
P- N/O-$C_{carbonyl}$	120.96(7)	120.90(9)	118.91(12)
N-$C_{carbonyl}$-O	121.89(11)	125.00(13)	118.16(17)

Table 2

Selected bond lengths (Å) and angles (°) of **2a**, **2b**, **3a^{II}** and **3b^{II}**.

	2a	**2b**	**3a^{II}**	**3b^{II}**
Ru1-P1	2.2956(6)	2.3432(7)	2.2005(6)	2.2186(5)
Ru1-P2	2.3057(6)	2.3068(7)	2.1925(7)	2.2196(5)
Ru1-P3	2.4935(6)	2.4481(8)		
Ru1-O1	2.1593(15)	2.1821(19)	2.1354(17)	2.1720(15)
Ru1-O2			2.1476(18)	2.1689(15)
Ru1-Cl1	2.4132(6)	2.4152(7)	2.3681(7)	2.4042(6)
Ru1-Cl2	2.4244(6)	2.4180(7)	2.4093(7)	2.4071(6)
P1-N1	1.757(2)	1.736(2)	1.746(2)	1.739(2)
P2-N2			1.771(2)	1.749(2)
P1-C	1.830(2)	1.829(3)	1.816(3)	1.822(2)
	1.845(2)	1.840(3)	1.826(3)	1.828(2)
P2-C			1.817(3)	1.818(2)
			1.830(3)	1.836(2)
$C_{carbonyl}$-N	1.356(3)	1.363(4)	1.354(3)	1.366(3)
			1.356(3)	1.366(3)
$C_{carbonyl}$-O	1.247(3)	1.247(3)	1.249(3)	1.241(3)
			1.243(3)	1.242(3)
P1-Ru1-O1	79.56(4)	80.00(6)	81.40(5)	83.56(4)
P2-Ru1-O2			81.61(5)	83.63(4)
P3-Ru1-O1	83.54(4)	82.89(6)		
P1-Ru1-P2	97.65(2)	98.03(3)	105.71(2)	103.26(2)
P2-Ru1-P3	100.48(2)	99.35(3)		
P1-Ru1-P3	159.31(2)	161.16(3)		
Cl1-Ru-Cl2	167.74(2)	170.71(3)	169.59(3)	165.81(2)
P1-Ru-O2	172.71(4)	177.11(6)	172.01(5)	172.97(4)
P2-Ru-O1			172.63(5)	172.65(4)
C-P1-C	103.16(10)	103.93(13)	104.92(12)	101.52(10)
C-P2-C			102.50(12)	99.24(10)
C-P1-N1	95.19(10)	96.73(13)	97.13(11)	102.05(10)
	103.50(10)	103.26(12)	104.31(12)	103.21(10)
C-P2-N2			99.33(12)	102.76(9)
			104.97(11)	103.72(10)
P-N-$C_{carbonyl}$	115.81(15)	117.69(19)	115.08(17)	117.86(14)
			116.17(17)	117.36(14)
N-C-O	121.9(2)	123.7(3)	121.8(2)	124.3(2)
			122.5(2)	124.7(2)

Table 3

Selected bond lengths (Å) and angles (°) of **3c^{I}** and **3c^{II}**.

	3c^{I}	**3c^{II}**
Ru1-P1	2.220(1) - 2.224(1)	2.2142(6)
Ru1-P2	2.213(1) - 2.220(1)	2.2153(7)
Ru1-N1	2.185(3) - 2.192(3)	2.191(2)
Ru1-N2	2.085(3) - 2.092(3)	2.141(2)
Ru1-Cl1	2.476(1) - 2.484(1)	2.4106(6)
Ru1-Cl2	2.421(1) - 2.428(1)	2.4143(6)
P1-O1	1.674(3) - 1.686(3)	1.679(2)
P2-O2	1.673(3) - 1.675(3)	1.685(2)
C1-N1	1.336(6) - 1.345(5)	1.345(3)
C18-N2	1.331(5) - 1.340(5)	1.335(3)
C1-O1	1.343(5) - 1.350(6)	1.362(3)
C18-O2	1.354(5) - 1.363(5)	1.365(3)
P1-Ru1-N1	79.76(9) - 79.84(9)	77.33(6)
P2-Ru1-N2	80.94(21) - 81.22(9)	77.92(6)
P1-Ru1-P2	98.07(4) - 98.38(4)	104.98(2)
Cl1-Ru-Cl2	89.41(4) - 91.65(4)	166.46(2)
P1-Ru-N2	89.73(10) - 90.02(9)	174.11(6)
P2-Ru-N1	176.40(8) - 176.93(9)	177.12(6)
P1-O1-C1	118.2(3) - 119.4(4)	114.7(2)
P2-O2-C18	117.8(3) - 118.0(2)	114.4(2)
N1-C1-O1	118.0(4) - 118.7(4)	118.4(2)
N2-C18-O2	118.4(4) - 118.7(3)	118.1(2)

Table 4

Energy differences (in kcal/mol) of isomers of the Ruthenium bis-chelates [$RuCl_2$(**L**)$_2$] for the herein reported ligands **L** = **1a**, **1b** and **1c**. Energy values of the crystallographically characterized isomers are written in bold style.

	1a	**1b**	**1c**
3^{I}	7.02	5.18	**0.00**
3^{II}	**0.00**	**0.00**	**2.40**
3^{III}	9.71	11.24	12.01
3^{IV}	11.82	12.23	9.98
3^{V}	16.08	20.71	2.29

Acknowledgements

R.G. is grateful to the Studentenwerk Freiberg and the Free State of Saxony for a Ph.D. scholarship (Landesgraduiertenstipendium).

Appendix A. Supplementary data

CCDC 1470582 (**1c**), 1470583 (**2b**·2.59 $CHCl_3$), 1470584 (**2a**·0.5 Et_2O), 1470585 (**3c^{I}**·2 $CHCl_3$), 1470586 (**3c^{II}**·CH_2Cl_2), 1470587 (**3b^{II}**·2 CH_2Cl_2), 1470588 (**3b^{II}**·7 $CHCl_3$), 1470589 (**3a^{II}**), 1470590 (**1b**), 1470591 (**1a**), 1470592 ($[RuCl_2(PPh_3)_3]$·MeOH) and 1470593 (phthalimidine, **HLb**) contain the supplementary crystallographic data for this article. These data can be obtained free of charge via http://www.ccdc.cam.ac.uk/conts/retrieving.html, or from the Cambridge Crystallographic Data Centre, 12 Union Road, Cambridge CB2 1EZ, UK; fax: (+44) 1223-336-033; or e-mail: deposit@ccdc.cam.ac.uk. Supplementary data associated with this article (that is: atomic coordinates and color graphics of the optimized molecular structures of **1a**, **1b**, **3a^{I}**, **3a^{II}**, **3a^{III}**, **3a^{IV}**, **3a^{V}**, **3b^{I}**, **3b^{II}**, **3b^{III}**, **3b^{IV}**, **3b^{V}**, **3c^{I}**, **3c^{II}**, **3c^{III}**, **3c^{IV}**and **3c^{V}**; Natural Charges of the atoms of **1a** and **1b**; color ORTEP diagrams of phthalimidine, $[RuCl_2(PPh_3)_3]$ in the mono-methanol solvate and **3b^{II}** in the hepta-chloroform solvate as well as tables with selected parameters of X-ray diffraction data collection and structure refinement) can be found, in the online version, at…

References

[1] J. Zhang, T.B. Gunnoe, J.L. Petersen, Inorg. Chem. 44 (2005) 2895.

[2] L. Villalobos, Z. Cao, P.E. Fanwick, T. Ren, Dalton Trans. 41 (2012) 644.

[3] L.O. de la Tabla, I. Matas, P. Palma, E. Álvarez, J. Cámpora, Organometallics 31 (2012) 1006.

[4] D. Matt, N. Sutter-Beydoun, A. El Amiri, J.-P. Brunette, P. Briard, D. Grandjean, Inorg. Chim. Acta 208 (1993) 5.

[5] D. Matt, M. Huhn, M. Bonnet, I. Tkatchenko, U. Englert, W. Kläui, Inorg. Chem. 34 (1995) 1288.

[6] C. Loeber, C. Wiesner, D. Matt, A. De Cian, J. Fischer, L. Toupet, Bull. Soc. Chim. Fr. 132 (1995) 166.

[7] K. Junge, B. Wendt, F.A. Westerhaus, A. Spannenberg, H. Jiao, M. Beller, Chem. Eur. J. 18 (2012) 9011.

[8] P. Braunstein, B.T. Heaton, C. Jacob, L. Manzi, X. Morise, Dalton Trans. (2003) 1396.

[9] A. Bader, E. Lindner, Coord. Chem. Rev. 108 (1991) 27.

[10] T. Miura, I.E. Held, S. Oishi, M. Naruto, S. Saito, Tetrahedron Lett. 54 (2013) 2674.

[11] K. Iida, T. Miura, J. Ando, S. Saito, Org. Lett. 15 (2013) 1436.

[12] R. Langer, A. Gese, D. Gesevičius, M. Jost, B.R. Langer, F. Schneck, A. Venker, W. Xu, Eur. J. Inorg. Chem. (2015) 696.

[13] M. Agostinho, V. Rosa, T. Avilés, R. Welter, P. Braunstein, Dalton Trans. (2009) 814.

[14] H.L. Milton, M.V. Wheatley, A.M.Z. Slawin, J.D. Woollins, Polyhedron 23 (2004) 3211.

[15] N. Otto, T. Opatz, Beilstein J. Org. Chem. 8 (2012) 1105.

[16] P. Cheshire, A.M.Z. Slawin, J.D. Woollins, Inorg. Chem. Commun. 5 (2002) 803.

[17] M.H. Norman, D.J. Minick, G.C. Rigdon, J. Med. Chem. 39 (1996) 149.

[18] S. Hanada, T. Ishida, Y. Motoyama, H. Nagashima, J. Org. Chem. 72 (2007) 7551.

[19] G.M. Sheldrick, Acta Crystallogr. A64 (2008) 112.

[20] G.M. Sheldrick, Acta Crystallogr. C71 (2015) 3.

[21] Gaussian 09, Revision D.01, M. J. Frisch, G. W. Trucks, H. B. Schlegel, G. E. Scuseria, M. A. Robb, J. R. Cheeseman, G. Scalmani, V. Barone, B. Mennucci, G. A. Petersson, H. Nakatsuji, M. Caricato, X. Li, H. P. Hratchian, A. F. Izmaylov, J. Bloino, G. Zheng, J. L. Sonnenberg, M. Hada, M. Ehara, K. Toyota, R. Fukuda, J. Hasegawa, M. Ishida, T. Nakajima, Y. Honda, O.

Kitao, H. Nakai, T. Vreven, J. A. Montgomery, Jr., J. E. Peralta, F. Ogliaro, M. Bearpark, J. J. Heyd, E. Brothers, K. N. Kudin, V. N. Staroverov, T. Keith, R. Kobayashi, J. Normand, K. Raghavachari, A. Rendell, J. C. Burant, S. S. Iyengar, J. Tomasi, M. Cossi, N. Rega, J. M. Millam, M. Klene, J. E. Knox, J. B. Cross, V. Bakken, C. Adamo, J. Jaramillo, R. Gomperts, R. E. Stratmann, O. Yazyev, A. J. Austin, R. Cammi, C. Pomelli, J. W. Ochterski, R. L. Martin, K. Morokuma, V. G. Zakrzewski, G. A. Voth, P. Salvador, J. J. Dannenberg, S. Dapprich, A. D. Daniels, O. Farkas, J. B. Foresman, J. V. Ortiz, J. Cioslowski, and D. J. Fox, Gaussian, Inc., Wallingford CT, 2013.

[22] NBO 5.G. E. D. Glendening, J. K. Badenhoop, A. E. Reed, J. E. Carpenter, J. A. Bohmann, C. M. Morales, and F. Weinhold (Theoretical Chemistry Institute, University of Wisconsin, Madison, WI, 2001); http://www.chem.wisc.edu/~nbo5

[23] Gaussian 03, Revision D.02, M. J. Frisch, G. W. Trucks, H. B. Schlegel, G. E. Scuseria, M. A. Robb, J. R. Cheeseman, J. A. Montgomery, Jr., T. Vreven, K. N. Kudin, J. C. Burant, J. M. Millam, S. S. Iyengar, J. Tomasi, V. Barone, B. Mennucci, M. Cossi, G. Scalmani, N. Rega, G. A. Petersson, H. Nakatsuji, M. Hada, M. Ehara, K. Toyota, R. Fukuda, J. Hasegawa, M. Ishida, T. Nakajima, Y. Honda, O. Kitao, H. Nakai, M. Klene, X. Li, J. E. Knox, H. P. Hratchian, J. B. Cross, V. Bakken, C. Adamo, J. Jaramillo, R. Gomperts, R. E. Stratmann, O. Yazyev, A. J. Austin, R. Cammi, C. Pomelli, J. W. Ochterski, P. Y. Ayala, K. Morokuma, G. A. Voth, P. Salvador, J. J. Dannenberg, V. G. Zakrzewski, S. Dapprich, A. D. Daniels, M. C. Strain, O. Farkas, D. K. Malick, A. D. Rabuck, K. Raghavachari, J. B. Foresman, J. V. Ortiz, Q. Cui, A. G. Baboul, S. Clifford, J. Cioslowski, B. B. Stefanov, G. Liu, A. Liashenko, P. Piskorz, I. Komaromi, R. L. Martin, D. J. Fox, T. Keith, M. A. Al-Laham, C. Y. Peng, A. Nanayakkara, M. Challacombe, P. M. W. Gill, B. Johnson, W. Chen, M. W. Wong, C. Gonzalez, and J. A. Pople, Gaussian, Inc., Wallingford CT, 2004.

[24] A.P. Shaw, B.L. Ryland, J.R. Norton, D. Buccella, A. Moscatelli, Inorg. Chem. 46 (2007) 5805.

[25] L.A. Ortiz-Frade, L. Ruiz-Ramírez, I. González, A. Marín-Becerra, M. Alcarazo, J.G. Alvarado-Rodriguez, R. Moreno-Esparza, Inorg. Chem. 42 (2003) 1825.

[26] E. Mothes, S. Sentets, M. Asuncion Luquin, R. Mathieu, N. Lugan, G. Lavigne, Organometallics 27 (2008) 1193.

[27] P. Braunstein, C. Frison, X. Morise, R.D. Adams, J. Chem. Soc., Dalton Trans. (2000) 2205.

[28] M.S. Balakrishna, D. Suresh, P. Kumar, J.T. Mague, J. Organomet. Chem. 696 (2011) 3616.

[29] S.J. La Placa, J.A. Ibers, Inorg. Chem. 4 (1965) 778.

[30] A.R. Cowley, J.R. Dilworth, C.A.M. von Beckh W., Acta Cryst. E61 (2005) m1237.

[31] H. Samouei, F.M. Miloserdov, E.C. Escudero-Adán, V.V. Grushin, Organometallics 33 (2014) 7279.

[32] R.D. Ernst, R. Basta, A.M. Arif, Z. Krist - New Cryst. St. 218 (2003) 49.

[33] P. Braunstein, D. Matt, Y. Dusausoy, Inorg. Chem. 22 (1983) 2043.

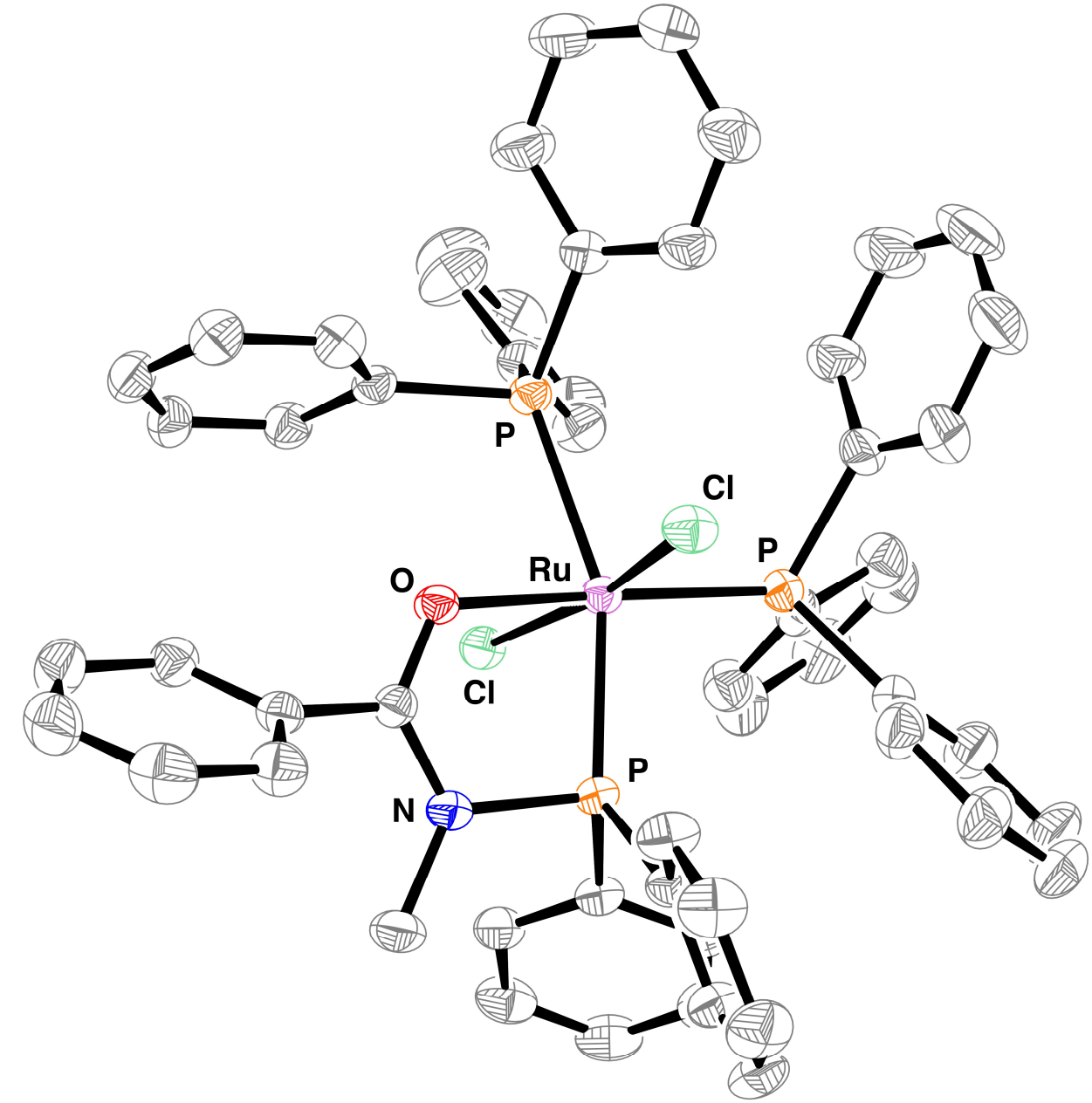

Graphical abstract

Graphical Abstract, Synopsis:

The chelating properties of ambidentate phosphane ligands with carboxylic amide motif were studied in the coordination sphere of Ru(II). These ligands act as P,N- or P,O-chelators with formation of octahedral mono- and bis-chelate Ru complexes.